Modeling of the Handover Dwell Time in Cellular Mobile Communications Systems

Marina Ruggieri, *Senior Member, IEEE*, Fabio Graziosi, *Member, IEEE*, and Fortunato Santucci, *Member, IEEE*

***Abstract*—In recent years, handover request queueing has been extensively analyzed as a handover protection scheme for future cellular networks. In this frame, however, while channel holding time distribution and cell boundary crossing rate have been modeled, the distribution of the allowed queue waiting time—i.e., the *handover dwell time*—has remained an open question from the modeling standpoint. In this frame, this paper proposes a model of the handover dwell time in circular cells coverage. The agreement between modeling and simulation results is very satisfactory. A fitting of an asymptotic behavior of the handover dwell-time distribution with a truncated Gaussian function is also provided, measuring the fitting goodness in various test cases. The practical insights the model can provide are also outlined in the paper.**

***Index Terms*—Cellular systems, handover area, handover dwell time, modeling and fitting.**

I. Introduction

IN FUTURE cellular mobile networks, the achievement of capacities much higher than the current ones will call for the deployment of small cells and, hence, for reliable handover procedures. In recent years, an extensive activity has been performed to identify optimal solutions for handover algorithms in future cellular networks, following both simulation-based and analytical approaches (e.g., [1]–[10]). In particular, protection schemes have been proposed for handover requests. These schemes are based on the use of reserved channels, queueing of handover requests or directed retry of handover attempts [2], [3], [6]–[8]. If no channel is immediately available in the target cell, both queueing and directed retry of handover requests benefit of a time interval, during which new calls are blocked and the mobile terminal (MT) is usually able to communicate with the current base station (BS), although the handover necessity has been already recognized. Those protection schemes result in a significant reduction of the handover failure probability at the expense of a usually acceptable increase in the blocking probability of new calls [2], [3], [6]–[8]. Results of extensive analytical approaches have been reported [2], [3], [9], [11]. In those papers, queue models with abandon have been considered to account for the limited waiting time allowed to queued handover requests. However, while the probability density functions of channel holding time and cell boundary crossing rate assumed therein are motivated by the results of specific analyses, the distribution of the allowed queue waiting time, i.e., the *handover dwell time*, has been only reasonably assumed [2], [3], [9], hence, representing an open question from the modeling standpoint. In particular, in the analysis described in [2], [3], and [9], an exponential and Gaussian distribution of the handover dwell time are assumed, respectively. However, as the handover dwell time represents an important parameter in the design of reliable handover schemes, a comprehensive characterization of its distribution is the only effective approach for its useful exploitation in the assessment of future cellular networks.

In the above frame, the authors have addressed the problem of modeling the handover dwell-time distribution. Some results were presented in recent works [12], [13]. On this basis, the present paper aims to modelize the handover dwell time by formulating its probability distribution under quite general assumptions. Mobility and propagation characteristics are included. The modeling results are reported and compared with those obtained by simulations. A very satisfactory agreement is found. Furthermore, a fitting of the handover dwell-time distribution with a truncated Gaussian function is proposed under asymptotic conditions for system parameters. The measures of fitting goodness in various test cases are reported.

The paper is organized as it follows: in Section II the adopted system model is described. Section III, which presents the handover dwell-time model, is organized in three sections: Section III-A reports the analysis under only mobility and geometry effects, and Sections III-B and III-C provide the model in the presence of shadow fading. In Section IV, model results are presented, discussed, and compared with those obtained by simulations. In Section V, a fitting of the handover dwell-time distribution with a truncated Gaussian function is described together with the achieved results. Finally, in Section VI, conclusions are drawn, and future perspectives of the work are outlined.

II. System Model

The service area is assumed to be regularly covered by circular cells. Intercell handovers of ongoing calls are considered to take place for MT's as they cross the border between adjacent cells. Once the initiation phase of a handover has been completed through absolute or relative measurements and a target BS has been selected, the *handover dwell time* T_d can be defined as *"the time interval the MT can spend communicating to the cell it is leaving (current cell) until the channel quality undergoes a minimum threshold."* Therefore, if a handover request is queued in the target cell when no

Manuscript received December 15, 1995; revised September 8, 1996.

M. Ruggieri is with the Department of Electronics Engineering, University of Roma Tor Vergata, I-00133 Rome, Italy.

F. Graziosi and F. Santucci are with the Department of Electrical Engineering, University of L'Aquila, I-67040 L'Aquila, Italy.

Publisher Item Identifier S 0018-9545(98)00680-X.

0018–9545/98$10.00 © 1998 IEEE

Authorized licensed use limited to: Indraprastha Institute of Information Technology. Downloaded on December 09,2023 at 08:17:43 UTC from IEEE Xplore. Restrictions apply.

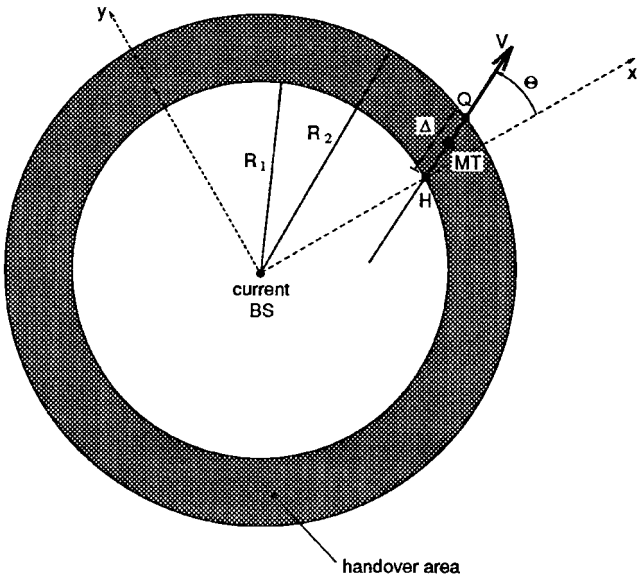

Fig. 1. Geometry and mobility parameters of the model.

channel is immediately available, the handover dwell time is the *allowed queue waiting time*.

In Fig. 1, the modeled configuration is depicted for the *current cell*. Further geometrical details are fully explained in Appendix A. A circular cell shape has been assumed and—as a first step—radio channel impairments—i.e., fadings—are neglected. On the inner circle in Fig. 1, the MT, which is leaving the *current cell*, experiences a channel quality $Q_{\rm ho}$ yielding to the recognition of the handover necessity. The outer circle corresponds to the lowest quality threshold $Q_{\rm th}$. It is here assumed that in intercell handovers channel quality is determined by the signal power the MT receives from the current BS, hence, $Q_{\rm ho}$ (handover threshold) and $Q_{\rm th}$ (quality threshold) represent signal power levels.

If only the mean path loss of the radio channel is accounted for, the handover dwell-time behavior depends on the terminal speed (module and direction) and on the *handover residual margin*, $M_{\rm HO}$ (decibels), given by the difference between $Q_{\rm ho}$ and $Q_{\rm th}$. When accounting for channel impairments, the down crossing of $Q_{\rm th}$ does not only depend on geometrical and mobility parameters, but it depends also on fading characteristics. In the latter case, T_d can be more properly defined as the *"time interval elapsed before the first down crossing of $Q_{\rm th}$ is experienced by the power level an active terminal receives from the current base station."* The latter definition addresses the level-crossing problem of random processes. It is reasonable to account only for shadowing, while neglecting fast fading effects. Indeed, since conditions for active call terminations are to be identified, the crossing events produced by fast fading determine short fading intervals and, hence, can be neglected.

The signal power level the MT receives from the current BS is a random process, which is here denoted by $L(t)$. It is modeled as

$$L(t) = k_1 - k_2 \log[d_{\rm BM}(t)] + A[d_{\rm BM}(t)] \tag{1}$$

where k_1 and k_2 are the mean path-loss coefficients, $d_{\rm BM}(t)$ is the time-dependent base to mobile distance, and $A[d_{\rm BM}(t)]$ denotes the shadow fading. The latter is characterized as a zero-mean Gaussian process, with exponentially decaying autocorrelation function [14]

$$\begin{aligned} R_A(t_2 - t_1) &= E\{A[d_{\rm BM}(t_2)]A[d_{\rm BM}(t_1)]\} \\ &= \sigma_A^2 \exp\left\{-\frac{|d_{\rm BM}(t_2) - d_{\rm BM}(t_1)|}{\bar{d}}\right\} \end{aligned} \tag{2}$$

where σ_A^2 is the variance of the shadowing and $\bar{d}$ is the typical autocorrelation decay distance.

III. Handover Dwell-Time Modeling

The model is developed in two steps: by first considering the radio channel only through the mean path loss (Section A) and then accounting also for shadowing effects (Sections B and C).

A. Modeling Under Geometry and Mobility Effects

In the geometrical configuration depicted in Fig. 1, R_1 represents the distance between the current BS and the point where the MT, which moves along a straight line, issues a handover request: hence, that distance corresponds to the down crossing of the threshold $Q_{\rm ho}$ by the received power level—R_2 represents the distance corresponding to the threshold $Q_{\rm th}$. Therefore, the difference $\Delta_R = R_2 - R_1$ is the depth of the handover area along the cell radius, and it is related to the residual margin $M_{\rm HO}$, the propagation coefficient $k_2/10$, and R_1 as it follows [from (1)]:

$$\Delta_R = R_1\left(10^{\frac{M_{\rm HO}}{k_2}} - 1\right). \tag{3}$$

Due to the random direction Θ of the MT motion, the distance Δ, i.e., the handover area depth along the direction Θ, can be expressed through the following relationship:

$$\Delta^2 = (x - R_1)^2 + y^2. \tag{4}$$

Then, it turns out to be a random variable, which through geometrical considerations (see Appendix A), can be expressed as a function of Θ, with R_1 and R_2 as parameters

$$\Delta^2(P) = \frac{R_2^2(1+P^2) + R_1^2(1-P^2) - 2R_1\sqrt{R_2^2(1+P^2) - R_1^2P^2}}{1+P^2} \tag{5}$$

where $P = \tan(\Theta)$. Therefore, indicating with V the MT speed, the handover dwell time is given by the straightforward expression

$$T_d = \frac{\Delta(P)}{V}. \tag{6}$$

V is considered to be a random variable too. Assuming that V and P are independent variables, their joint probability density function $f_{V,P}(v,p)$ can be expressed through their marginal density functions $f_V(v)$ and $f_P(p)$, respectively, as follows:

$$f_{V,P}(v,p) = f_V(v)f_P(p) \tag{7}$$

Authorized licensed use limited to: Indraprastha Institute of Information Technology. Downloaded on December 09,2023 at 08:17:43 UTC from IEEE Xplore. Restrictions apply.

where v and p indicate the determinations of V and P, respectively. Hence, the mean value of the handover dwell time T_d can be directly evaluated as

$$E\{T_d\} = \int\int_{V,P} \frac{\Delta(p)}{v} f_V(v) f_P(p)\, dv\, dp = \int_V \frac{f_V(v)}{v}\, dv \int_P \Delta(P) f_P(p)\, dp \tag{8}$$

while the probability density function of T_d can be derived through the use of an auxiliary variable $W = P$ [15]

$$f_{T_d}(t_d) = \int_W f_{T_d,W}(t_d, w)\, dw = \int_W f_V\left(\frac{\delta(w)}{t_d}\right) f_P(w) \frac{\delta(w)}{t_d^2}\, dw \tag{9}$$

where t_d, w, and $\delta(w)$ denote the determinations of the random variables T_d, W, and $\Delta(W)$, respectively.

B. Modeling Under Shadowing Effects

When the effects of shadow fading are accounted for in order to modelize an actual cellular environment, the dwell-time distribution depends on the sequence of signal levels that the MT receives from its current BS. In particular, a quality estimate can be carried out on the communication link through proper averages of the signal levels measured by the MT at regular time intervals T. Those averages are compared to the quality threshold in order to verify whether the link quality is still acceptable or not at the end of each time interval T. The statistics of the averaged process can be related to the outage probability experienced within the handover dwell-time interval. The latter problem is beyond the aims of this paper. Moreover, it is here assumed that the same average of the received signal is used to detect the handover, thus considering an initiation algorithm based on absolute measurements. This means that the first down crossing of $Q_{\rm ho}$ yields handover detection, while the first down crossing of $Q_{\rm th}$ by the same process yields forced termination detection. Such an assumption does not limit the validity of the following analysis. In fact, a handover algorithm is usually based on absolute measurements combined to other algorithms (e.g., relative measurements) to reduce flip flopping between BS's belonging to adjacent cells [16]. Moreover, in order to characterize more properly the effects of shadow fading, in what follows, terminal mobility is restricted to the motion along a radial straight line from the current BS (i.e., $\Theta = 0$ in Fig. 1), and a constant speed module $V = v$ is assumed. In this frame, assuming also that the MT starts moving from the current BS at $t = 0$, a discrete time version $L(nT)$ of the received signal level can be introduced

$$L(nT) = k_1 - k_2 \log(nvT) + A(nvT). \tag{10}$$

By averaging $L(nT)$, the process $X(nT)$ is obtained

$$X(nT) = L(nT) \otimes h(nT) = [k_1 - k_2 \log(nvT) + A(nvT)] \otimes h(nT) \tag{11}$$

where $\otimes$ indicates a discrete convolution and $h(nT)$ is the real valued impulse response of a finite-impulse response (FIR) filter, which performs a normalized average over M samples. In particular, denoting by $w(nT)$ the generic averaging window of length M, $h(nT)$ is given by

$$h(nT) = \frac{w(nT)}{NT} \tag{12}$$

where

$$N = \sum_{n=0}^{M-1} w(nT). \tag{13}$$

The mean and autocovariance function of $X(nT)$ can be derived as

$$m_X(nT) = E\{L(nT)\} \otimes h(nT) = [k_1 - k_2 \log(nvT)] \otimes h(nT) \tag{14}$$

$$C_X(nT) = C_A(nT) \otimes h(nT) \otimes h(-nT) \tag{15}$$

where $C_A(nT)$ and $C_X(nT)$ indicate the autocovariance functions of $A(nvT)$ and $X(nT)$, respectively.

Moreover, the variance and the correlation coefficient between two random variables, taken from $X(nT)$ at the time instants nT and $(n+1)T$, are given by

$$\sigma_X^2 = C_X(0) \tag{16}$$

$$\rho_X = \frac{C_X(T)}{\sigma_X^2}. \tag{17}$$

The effects of shadow fading on the handover dwell-time distribution are accounted for by applying the level-crossing theory of Gaussian processes to determine the first down-crossing event of the quality threshold. In this case, assuming $M_{\rm HO}$ larger enough than σ_X, the series of crossing events of $Q_{\rm th}$ can be regarded as a Poisson point process with an acceptable degree of approximation. The choice of the first down-crossing event for determining the boundary of the handover dwell area is reasonable [10], [17]. It is to be remarked that $X(nT)$ is nonstationary, due to the time dependence of its mean value. Therefore, according to [1], [18], and [19], the series of crossing events can be regarded as a variable rate Poisson point process within each time interval where the process stationarity can be assumed. The range of stationarity clearly depends on T, v, and cell size R_1, the latter being a function of k_2. Starting from the down-crossing probability for Gaussian processes within a time interval T approaching zero [15], [18], the mass probability function of the handover dwell time can be expressed through the probability that a single down crossing occurs in the generic time interval $[kT, (k+1)T)$. Due to the Poisson point process assumption, crossing events occurring in nonoverlapping intervals are independent.

The above remarks are firstly exploited to derive an analytical expression of the T_d probability mass function for a given time instant $t_{\rm ho} = k_0 T$ where the down crossing of $Q_{\rm ho}$ occurs. This means that the model moves from $t_{\rm ho}$ to evaluate the probability of down crossing of the threshold $Q_{\rm th}$. Hence,

Authorized licensed use limited to: Indraprastha Institute of Information Technology. Downloaded on December 09,2023 at 08:17:43 UTC from IEEE Xplore. Restrictions apply.

for a small T the probability mass function of the handover dwell time $p_{T_d}(kT)$ can be written as

$$p_{T_d}(k_dT) = P_{1,u}(kT) \prod_{j=k_0}^{k-1} \{1 - P_{1,u}(jT)\} \qquad (18)$$

where $P_{1,u}(kT)$ is the probability of down crossing once an arbitrary level u (in the present case $Q_{\rm th}$) within the time interval $[kT, (k+1)T)$ and $k_d = k - k_0 + 1$. In (18), it is assumed that

$$\prod_{h=i, i>j}^{j} \{\cdot\} = 1.$$

If $\rho_X \cong 1$, an approximate expression generally holds for $P_{1,u}(kT)$ [15, pp. 486 and 492]

$$P_{1,u}(kT) \cong \frac{\arccos[\rho_X]}{(2\pi)} \exp\left\{ -\frac{[m_X(kT) - u]^2}{2\sigma_X^2} \right\} \qquad (19)$$

with $k = k_0, k_0 + 1, \cdots$. Since (18) and (19) hold true for $\rho_X \cong 1$, a short enough T is required [15]. By using (14)–(17) in the evaluation of (19), the handover dwell-time distribution is finally obtained through (18).

In order to implement a recursive algorithm for evaluating the T_d mass probability, the expression of $p_{T_d}(k_dT)$ can be also given in the following form:

$$p_{T_d}(k_dT) = P_{1,u}(kT) \left\{ 1 - \sum_{j=0}^{k_d-1} p_{T_d}(jT) \right\}. \qquad (20)$$

In fact, by setting an initialization parameter $A_0 = 1$, the k_dth step $(k_d \geq 1)$ of the recursive formulation can be expressed as

$$\begin{cases} A_{k_d} = A_{k_d-1} - p_{T_d}[(k_d - 1)T] \\ p_{T_d}(k_dT) = P_{1,u}(kT) A_{k_d}. \end{cases} \qquad (21)$$

From all the above, it obviously results that $p_{T_d}(k_dT) = 0$ for $k_d \leq 0$. Actually, k_0T and the corresponding distance k_0vT from the current BS are also random variables, which can be characterized through (18)–(19) or (21) with $u = Q_{\rm ho}$ and $k = 0, 1, \cdots$, reasonably assuming that for $k = 0$, $E\{X(kT)\}$ is well above $Q_{\rm ho}$. A simplified approach has been followed in deriving k_0, taking k_0T as the time instant which maximizes the $Q_{\rm ho}$ down-crossing probability.

The proposed model involves two types of assumptions: 1) the local stationarity of the process $X(kT)$ and a correlation coefficient ρ_X close to one and 2) the Poisson point process assumption for the series of down-crossing events of the thresholds. In this frame, both $M_{\rm HO}$ and σ_A (the standard deviation of the process $L(t)$) are related to assumptions 2), while v and R_1 concerns both assumptions 1) and 2). In evaluating model performance, $M_{\rm HO}$ and σ_A are considered through the ratio $\sigma_X/M_{\rm HO}$. In fact, as $m_X(kT)$ decreases with kT, the Poisson point process approximation works satisfactorily if $[m_X(kT) - Q_{\rm th}]$ is larger than σ_X. Hence, in order to exploit effectively the Poisson approximation in the recursive model (19)–(21), σ_X is required to be sufficiently smaller than $M_{\rm HO}$.

As far as the parameter v is concerned, the local stationarity assumption calls for relatively small values of v. In fact, the validity of that assumption depends on the distance $d = vT$ between adjacent sampling points. Hence, it depends on the speed v for a given T. Moreover, small values of v would be also preferable to keep the correlation coefficient ρ_X close to one, as required to utilize (19) in the modeling. On the other hand, for a given averaging window, σ_X decreases when v increases, thus suggesting high values of v. However, numerical results will show that a suitable balance among these needs takes place in most cases. Finally, an increase of R_1 results in a smoother path loss within the handover area, hence improving the validity of the local stationarity assumption.

C. Modeling Under the Effects of Large Excursions

In this section, large excursions of the process $X(nT)$ are accounted for to complete the modeling of the handover dwell time in the presence of shadow fading [18], [20]. The model is developed by first considering the continuous time process $X(t)$, and then the application to its sampled form $X(nT)$ is provided. In Section III-B, the modeling was based on the first down-crossing event of the threshold $Q_{\rm th}$, assuming that the down crossing of $Q_{\rm ho}$ had already taken place. The Poisson assumption is very reasonable, as it is confirmed by the results displayed in Section IV, if the residual margin $M_{\rm HO}$ is sufficiently large (i.e., the thresholds $Q_{\rm ho}$ and $Q_{\rm th}$ are sufficiently spaced). In fact, in the latter case insights of the level-crossing theory are applicable to the Gaussian process $X(t)$. The intrinsic assumption is that the first down crossing of $Q_{\rm ho}$ (i.e., the initialization point) and the first down crossing of $Q_{\rm th}$ are sufficiently spaced (either in the time or in the distance domain). However, when the residual margin is "too close" to the standard deviation of $X(t)$, the first down crossing of $Q_{\rm ho}$ and the first down crossing of $Q_{\rm th}$ might belong to a same large excursion in the region where $m_X(t) = E\{X(t)\}$ is well above $Q_{\rm ho}$. In this case, the down crossing of $Q_{\rm ho}$ would be closely followed by the down crossing of $Q_{\rm th}$ (i.e., the same excursion would cause the contemporary crossing of $Q_{\rm ho}$ and $Q_{\rm th}$). The effects of large excursions of Gaussian processes are hence introduced in the modeling to extend its validity to low values of $M_{\rm HO}$. From [20], it results that the excursions of a zero-mean, unit-variance Gaussian process $Z(t)$ above or below a threshold Q (with $|Q| \geq 4$) show a parabolic behavior. In particular, the following asymptotic expression holds true in the large excursion region:

$$Z(t) = Q - \xi\sigma_{z'}t - \frac{1}{2}Q\sigma_{z'}^2t^2 \qquad (22)$$

where ξ is a Rayleigh-distributed random variable, $Z'(t)$ denotes the first time derivative of $Z(t)$, and $\sigma_{z'}^2$ is the power of $Z'(t)$. The asymptotic theory of large excursions is applied to the case of interest, where two close enough thresholds, $Q_{\rm ho}$ and $Q_{\rm th}$, are considered. In order to utilize the above parabolic approximation of large excursions, the following notation is

Authorized licensed use limited to: Indraprastha Institute of Information Technology. Downloaded on December 09,2023 at 08:17:43 UTC from IEEE Xplore. Restrictions apply.

adopted:

$$Q_1(t) \triangleq \frac{Q_{\rm ho} - m_X(t)}{\sigma_X}$$
$$Q_2(t) \triangleq \frac{Q_{\rm th} - m_X(t)}{\sigma_X} \tag{23}$$

and a zero-mean unit-variance process $Y(t)$ is defined

$$Y(t) \triangleq \frac{X(t) - m_X(t)}{\sigma_X}. \tag{24}$$

Let us denote by t_1 and t_2, respectively, the time instants corresponding to the down-crossing events of $Q_1(t)$ and $Q_2(t)$ by $Y(t)$ in a large excursion. Due to the slow decay of $m_X(t)$, if compared with the sharp decay of the fading component within a large excursion, it is assumed that $m_X(t)$ does not change significantly in the time interval interested by the excursion. Hence, $Q_1(t)$ and $Q_2(t)$ can be considered fairly constant in that interval ($Q_1(t) \cong Q_1(t_2)$ and $Q_2(t) \cong Q_2(t_2)$ for $t_1 \le t \le t_2$). Since $Q_1(t_2)$ and $Q_2(t_2)$ are close to each other, it is reasonably assumed that the parabolic behavior of $Y(t)$ still holds between $Q_1(t_2)$ and $Q_2(t_2)$. As a consequence, moving from (22), the time interval $\bar{t} = t_2 - t_1$ can be expressed as

$$\bar{t} = \frac{\xi - \sqrt{\xi^2 - 2Q_2(t_2)[Q_1(t_2) - Q_2(t_2)]}}{Q_2(t_2)\sigma_{z'}}. \tag{25}$$

Therefore, for a given t_2, the probability density function of the random variable $\bar{T}$, with determination $\bar{t}$, is found to be

$$f_{\bar{T}|T_2}(\bar{t} \mid t_2) = -\frac{Q_2^2(t_2)\sigma_{z'}^4\bar{t}^4 - 4[Q_1(t_2) - Q_2(t_2)]^2}{4\sigma_{z'}^2\bar{t}^3} \cdot \exp\left\{-\frac{\{Q_2(t_2)\sigma_{z'}^2\bar{t}^2 + 2[Q_1(t_2) - Q_2(t_2)]\}^2}{8\sigma_{z'}^2\bar{t}^2}\right\} \tag{26}$$

where the conditioning parameter t_2 represents a particular value of the random variable T_2. The latter is the random time instant corresponding to the down crossing of $Q_2(t)$. Finally, the probability density function of $\bar{T}$ can be obtained as follows:

$$f_{\bar{T}}(\bar{t}) = \frac{\int_0^{\bar{t}_1} f_{\bar{T}|T_2}(\bar{t} \mid \zeta) f_{T_2}(\zeta)\, d\zeta]}{\int_0^{\bar{t}_1} f_{T_2}(\zeta)\, d\zeta}. \tag{27}$$

In the above equation, $f_{T_2}(t_2)$ is the probability density function of T_2 and $\bar{t}_1$ is the time instant corresponding to the right-hand boundary of the interval where down crossings of $Q_1(t)$ more likely depend on large excursions. Beyond that point, it can be assumed that the level-crossing theory applies better than the large excursions approach. It is here assumed that $\bar{t}_1$ is the time instant which maximizes the probability of down crossing $Q_1(t)$.

Moreover, it can be noticed from (25) that for a given t_2, $\bar{t}$ is maximum at $\xi = 0$, that is,

$$\bar{t} \le \sqrt{\frac{2[Q_2(t_2) - Q_1(t_2)]}{Q_2(t_2)\sigma_{z'}^2}} = \sqrt{\frac{2[Q_{\rm th} - Q_{\rm ho}]}{[Q_{\rm th} - m_x(t_2)]\sigma_{z'}^2}}. \tag{28}$$

In the above inequality, the upper bound is maximum when t_2 approaches $\bar{t}_1$. Hence, it results

$$\bar{t}_{\max} = \sqrt{\frac{2(Q_{\rm th} - Q_{\rm ho})}{[Q_{\rm th} - m_x(\bar{t}_1)]\sigma_{z'}^2}}. \tag{29}$$

A discrete time model is then obtained by setting

$$k_{\max} \triangleq \lfloor \bar{t}_{\max}/T \rfloor \tag{30}$$

where $\lfloor x \rfloor$ represents the highest integer less than or equal to x. Through some analytical manipulations (see Appendix B), (31), given at the bottom of the page, finally results for the complete characterization of the handover dwell time, where $p_{T_2}(kT)$ denotes the probability mass function of T_2 and can be approximated as $p_{T_2}(kT) \simeq f_{T_2}(kT)T$. It can be noticed that when

$$p_{T_2}(jT) \cong 0 \quad \text{for } j = 0, 1, 2, \cdots, k_0 - 1 \tag{32}$$

i.e., when large excursions have a negligible effect, (31) approaches (18).

IV. Results

In this section, results obtained through the described model are presented. In particular, a parametric analysis has been performed in order to validate the modeling approach presented in Sections III-B and III-C in ranges of interest for the following system parameters: cell size, mobile speed, and channel characteristics.

A. Modeling Results Under Geometry and Mobility Effects

A regular macrocellular coverage is considered for numerical examples. Therefore, the random direction Θ of the MT motion is reasonably assumed to be uniformly distributed in $[-\pi/2, \pi/2]$ [21]. Hence, $P = \tan(\Theta)$ results to be a Cauchy-distributed random variable. Moreover, the speed module V follows a left-side truncated Gaussian distribution with mean $\bar{V}$ and variance σ_v^2.

For a given set of system parameters, numerical integration of (8) and (9) provides the mean value and the probability density function of the handover dwell time T_d, respectively. In particular, in Fig. 2(a) the probability density function of

$$p_{T_d}(k_dT) \cong \begin{cases} p_{T_2}[(k_d + k_0)T] \\ \quad + T\sum_{j=0}^{k_0} f_{\bar{T}|T_2}(k_dT \mid jT)p_{T_2}(jT), & \text{if } k_d = 1, \cdots, k_{\max} \\ p_{T_2}[(k_d + k_0)T], & \text{if } k_d = k_{\max} + 1 \\ & \quad k_{\max} + 2, \cdots. \end{cases} \tag{31}$$

Authorized licensed use limited to: Indraprastha Institute of Information Technology. Downloaded on December 09,2023 at 08:17:43 UTC from IEEE Xplore. Restrictions apply.

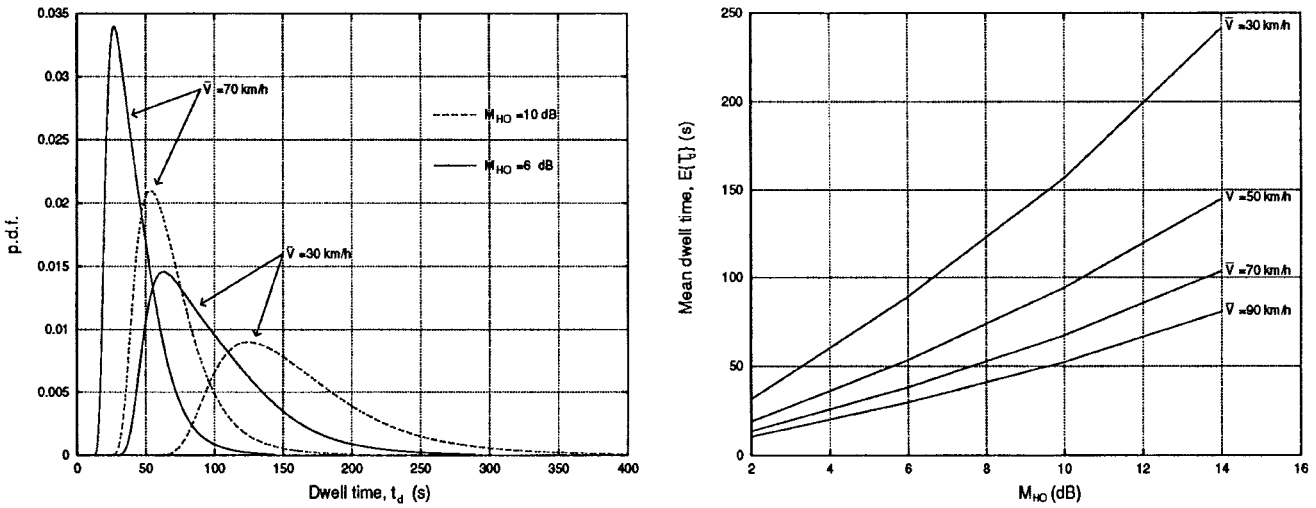

(a) (b)

Fig. 2. (a) Handover dwell-time probability function derived under geometry and mobility effects. (b) Mean handover dwell time versus $M_{\rm HO}$ as obtained under geometry and mobility effects ($\sigma_v = \bar{V}/4$ and $R_1 = 1$ km).

T_d is shown for a nominal cell radius $R_1 = 1$ km. The mean value $\bar{V}$ of the mobile speed and the residual margin $M_{\rm HO}$ are taken as parameters. It is assumed $\sigma_v = \bar{V}/4$ for the standard deviation of the mobile speed. It can be noticed that, due to the random direction of motion, the density function is not Gaussian. Moreover, if $\bar{V}$ is increased and/or $M_{\rm HO}$ is reduced, smaller values of T_d become more likely and the curves get sharper around their peak values. It can be also noticed that the probability of having very small T_d values is negligible, and, hence, a certain queueing interval is anyway allowed. It is straightforward that for increasing values of $\bar{V}$, a larger $M_{\rm HO}$ should be provided. However, this would cause an increase in the overlapping area percentage and a consequent increase in cochannel interference levels [22].

In Fig. 2(b), the mean value of T_d is displayed versus $M_{\rm HO}$ for different values of the mean mobile speed $\bar{V}$. It can be noticed that $E\{T_d\}$ increases more than linearly with $M_{\rm HO}$, as one should expect from the relationship (3) between Δ_R and $M_{\rm HO}$. Moreover, for increasing values of $M_{\rm HO}$, the distance between curves corresponding to different values of $\bar{V}$ also increases.

The above results have been obtained for a given value of R_1. The effect of cell radius can be accounted for by (3), where a linear dependence between Δ_R and R_1 is found. As a consequence, for a given value of $M_{\rm HO}$, the increase of R_1 yields an increase in the overlapping area and, hence, higher values of T_d become more likely. Therefore, for a given propagation environment (i.e., for a given value of k_2) and a given overlapping area percentage Δ_R/R_1 with respect to the nominal cell area (i.e., for a given value of $M_{\rm HO}$), the handover dwell time becomes less critical as R_1 gets larger.

B. Modeling Results Under Shadowing Effects

The results presented in this section have been obtained through (18)–(21) and (31). Simulations results are also reported for comparison, and the agreement is discussed. In what follows, it is assumed that $T = 480$ ms, $k_2 = 33.8$, and $\bar{d} = 20$ m. Moreover, a rectangular averaging window is adopted, i.e.,

$$h(nT) = \begin{cases} \frac{1}{MT}, & \text{if } 0 \le n \le M-1 \\ 0, & \text{elsewhere} \end{cases} \tag{33}$$

with $M = 20$.

Numerical results have been obtained for a wide range of system parameters, namely, cell radius R_1, residual handover margin $M_{\rm HO}$, shadow fading standard deviation σ_A, and mobile speed v. In Fig. 3(a), the probability mass function of T_d is shown for two values of R_1 and two values of $M_{\rm HO}$, assuming that $\sigma_A = 4$ dB and $v = 25$ km/h. It can be noticed that model and simulations are in close agreement. In particular, the agreement is better for $R_1 = 2$ km. In fact, by increasing cell radius, the local stationarity assumption for $X(t)$ holds better in the region where the down crossings of $Q_{\rm ho}$ and $Q_{\rm th}$ more likely occur. It can be also noticed that the agreement worsens on the right tails of the curves. In fact, the Poisson point process assumption loses validity in that region. As a consequence, (21) provides an overestimate of the $Q_{\rm th}$ crossing probability when $m_X(nT)$ becomes very close to the threshold. From Fig. 3(a), it can be also noticed that when R_1 increases, larger values of T_d become more likely and the same holds for $M_{\rm HO}$. Moreover, the curves become sharper as R_1 decreases, leading to a lower spread of the T_d values.

In Fig. 3(b), the effect of varying the mobile speed is explored. It obviously results that lower T_d values become more likely when the speed increases. Moreover, it can be noticed that model and simulations get in closer agreement for decreasing values of v. Indeed, the local stationarity assumption within an interval of duration T holds better for lower values of v. Moreover, the correlation coefficient ρ_X becomes closer to one, although σ_X tends to increase for decreasing values of v. However, the agreement is still satisfactory for speed values in ranges of practical interest.

In Fig. 4(a), results from model and simulations are presented for a smaller value of $M_{\rm HO}$. As it can be noticed, the effect of large excursions is pointed out by a spike in the low T_d region. The agreement between model and simulation is

Authorized licensed use limited to: Indraprastha Institute of Information Technology. Downloaded on December 09,2023 at 08:17:43 UTC from IEEE Xplore. Restrictions apply.

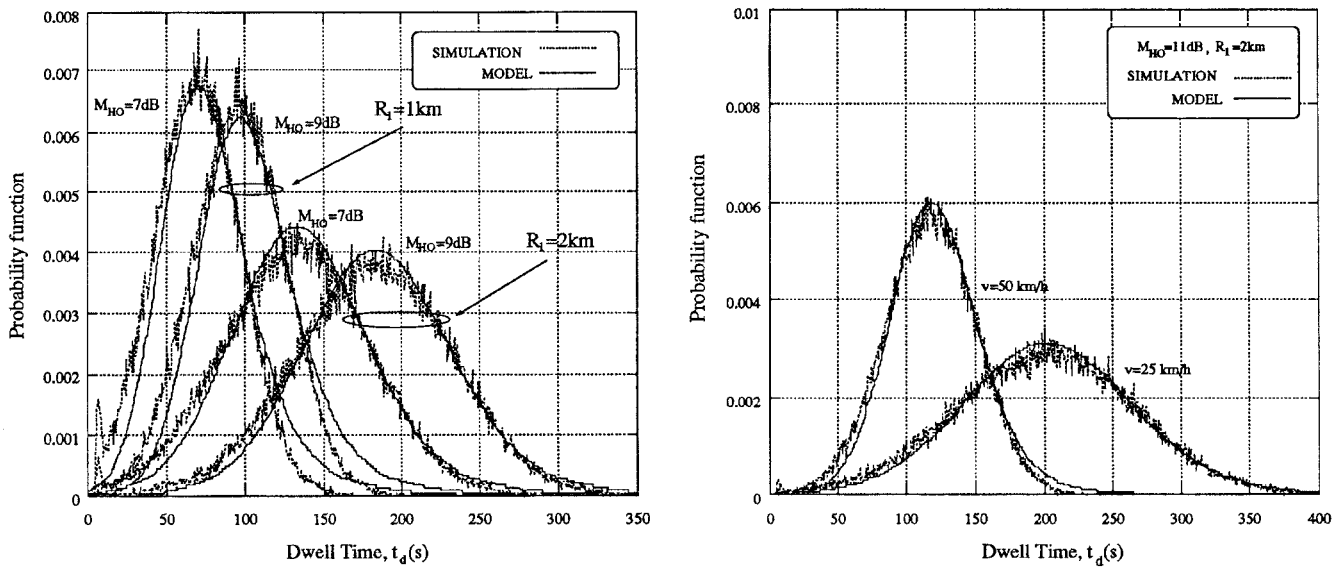

(a) (b)

Fig. 3. Handover dwell-time probability function derived under shadowing effects. (a) Comparison between model and simulation ($v = 25$ km/h and $\sigma_A = 4$ dB). (b) Effects of mobile speed ($R_1 = 2$ km and $\sigma_A = 4$ dB).

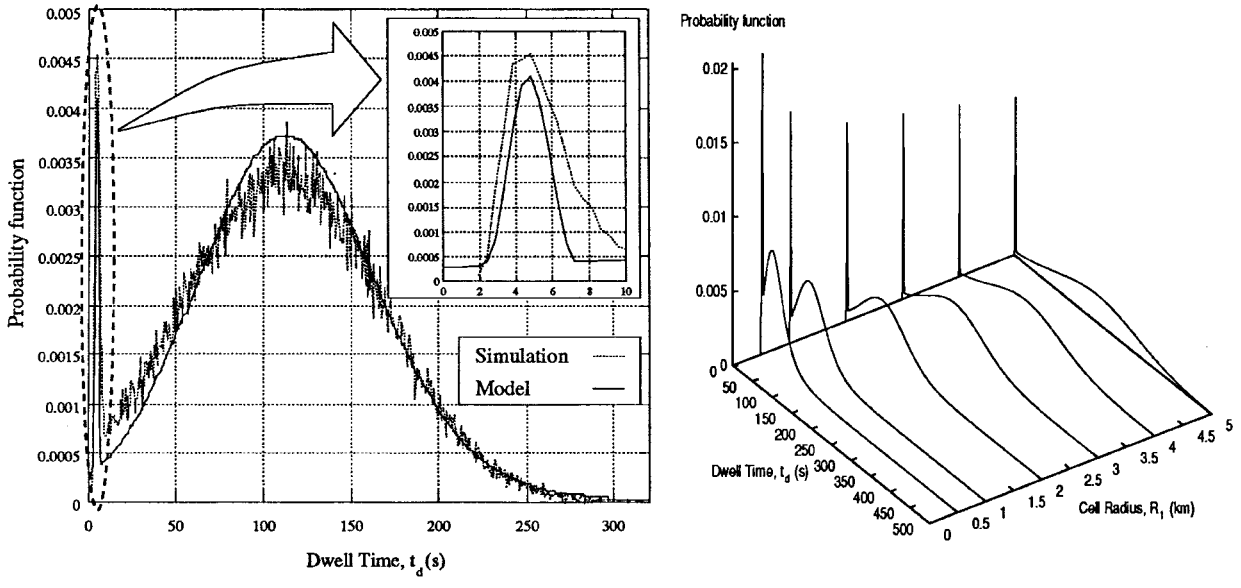

(a) (b)

Fig. 4. Handover dwell-time probability function derived under shadowing effects. (a) Effects of large excursions ($R_1 = 2$ km, $v = 25$ km/h, $M_{\rm HO} = 7$ dB, and $\sigma_A = 6$ dB). (b) Effects of cell size ($v = 25$ km/h, $M_{\rm HO} = 7$ dB, and $\sigma_A = 8$ dB).

still satisfactory, although a small difference exists only in the peak amplitude. In Fig. 4(b), the effect of varying R_1 is shown as obtained from the model in the presence of large excursions. It can be noticed that, for a given value of $M_{\rm HO}$, the spike amplitude varies with R_1, while its position is substantially unaffected by R_1. Moreover, when R_1 increases, the most regular part of the curve shifts to the right, while showing a larger spread.

A further remark concerns the practical insights the model can provide. If $M_{\rm HO}$ is large enough with respect to σ_X, low T_d values occur with small probability. Moreover, in a given propagation environment and for a given $M_{\rm HO}$—that means for a given percentage of the overlapping area—the handover dwell time is less critical when v decreases and/or R_1 increases. However, when $M_{\rm HO}$ decreases, low values of T_d become more likely. The probability of low T_d suddenly increases as large excursions occur. To this respect, in Table I the mean value of T_d is listed for different choices of system parameters. Moreover, the probability that a certain value of T_d is not exceeded is reported in the table in order to account for large excursions. In the same table, the values obtained from simulations are also reported. It can be noticed that the mean value obtained from the model and the one obtained from simulations are in better agreement when $M_{\rm HO}$ is large, i.e., when the effect of large excursions is negligible. On the other hand, a quite close agreement is found for $P\{T_d \leq 10\}$

Authorized licensed use limited to: Indraprastha Institute of Information Technology. Downloaded on December 09,2023 at 08:17:43 UTC from IEEE Xplore. Restrictions apply.

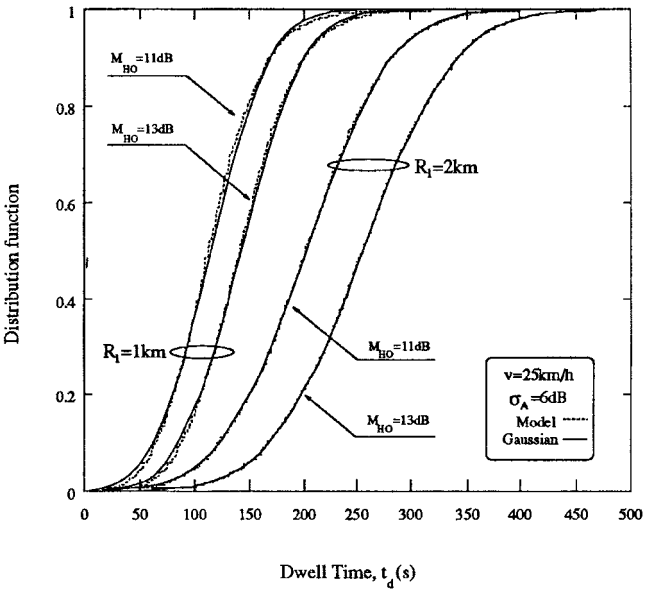

Fig. 5. Comparison between the distribution function obtained from the model and the fitting Gaussian distribution function. Various values of system parameters are considered.

TABLE I
SOME STATISTICAL PROPERTIES OF T_d AS OBTAINED FROM THE MODEL AND SIMULATIONS FOR VARIOUS SYSTEM PARAMETERS

			Model		Simulation	
R_1 (km)	M_{HO}(dB)	v (km/h)	E[T_d] (s)	P[T_d<10]	E[T_d] (s)	P[T_d<10]
1	3	25	34.11	0.4236	22.74	0.4478
1	5	25	50.11	0.1609	40.32	0.2068
1	13	25	143.78	0.0002	136.58	0.0013
1	3	50	17.36	0.4234	13.14	0.5160
1	5	50	26.96	0.1443	23.37	0.2375
1	13	50	84.60	0.00004	79.24	0.0004
2	3	25	51.57	0.3537	41.92	0.3651
2	5	25	81.25	0.1114	74.58	0.1307
2	13	25	256.26	0.00008	252.08	0.0003
2	3	50	31.61	0.3114	24.57	0.3524
2	5	50	49.37	0.0750	43.50	0.1218
2	13	50	152.29	0.000004	148.54	0.00006

when M_{HO} is small, i.e., when the effect of large excursions is significant. From the above, it appears that the margin M_{HO} is a critical parameter. In fact, the handover dwell-time distribution shows a nearly regular shape (the Gaussianity of such distribution is discussed in the next section) if M_{HO} is high enough. However, if M_{HO} is small, the probability of having very short T_d might be quite high, due to the effect of large excursions.

V. FITTING OF HANDOVER DWELL-TIME DISTRIBUTION

Both modeling and simulations results presented so far have clearly shown that for a certain set of system parameters and wide enough ranges of their value, the dwell-time distribution has a Gaussian-like shape. Then, this insight is hereinafter validated. In particular, simulation data have been submitted to the Kolmogorov–Smirnov test [15], [23]. The empirical distribution obtained from simulations (10 000 samples) has been compared to a Gaussian distribution which is truncated on its left side. Mean and variance of the distribution have been also estimated from simulation data. The results of the Kolmogorof–Smirnov test are shown in Table II in terms of values of the test random variable. It has been assumed a 5% significance level, which implies that the test variable must be lower than 0.0136 in order to overcome the test. The test condition is not satisfied only in one case, as it is shown in Table II. In general, the Gaussianity assumption holds true when large excursions are negligible, the agreement being closer as M_{HO} increases. The Gaussian approximation has been tested also with the model results by computing the integral G (from zero to ∞) of the normalized difference between the complementary distribution function obtained from the model and the Gaussian complementary distribution function, whose parameters have been estimated from the model itself [2]. The values of G are shown in the last column of Table II, for the same configurations submitted to the Kolmogorov–Smirnov test. As G is expected to approach one in the worst case and zero in the best case, the obtained values can be considered satisfactory.

TABLE II
KOLMOGOROV–SMIRNOV TEST RESULTS AND MEASURE OF FITTING GOODNESS

R_1 (km)	M_{HO}(dB)	v (km/h)	σ_A (dB)	σ_X (dB)	K-S test	G
1	11	25	4	2.61	0.007088	0.0544
1	13	25	4	2.61	0.009124	0.0266
1	13	25	6	3.92	0.006708	0.0112
1	13	50	8	4.06	0.004250	0.0492
2	9	25	4	2.61	0.006168	0.0061
2	11	25	4	2.61	0.007032	0.0032
2	13	25	4	2.61	0.009685	0.0018
2	11	25	6	3.92	0.012469	0.0027
2	13	25	6	3.92	0.008931	0.0015
2	7	50	4	2.03	0.016487	0.1802
2	11	50	6	2.03	0.007762	0.0121
2	13	50	8	4.06	0.005707	0.0056

In Fig. 5, the distribution function obtained through the model and the fitting Gaussian distribution function are shown and compared for various values of system parameters. A very satisfactory agreement is again obtained. Furthermore, it can be noticed that the agreement improves when both handover margin and cell size increase.

VI. CONCLUSION

The paper has proposed and described a model of the handover dwell time in cellular mobile systems. A circularly shaped cell geometry has been assumed and shadow fading effects have been included. The handover dwell-time probability function has been derived. The results achieved through the approach have provided a satisfactory agreement with those obtained by simulations.

The proposed model, which needs for a very low computational time (a few seconds) if compared with that of simulation runs (a few hours), is based on the theories of level crossing and large excursions of Gaussian processes.

Authorized licensed use limited to: Indraprastha Institute of Information Technology. Downloaded on December 09,2023 at 08:17:43 UTC from IEEE Xplore. Restrictions apply.

Under quite general assumptions, it is seen that the handover dwell time tends to be Gaussian distributed for high values of the handover residual margin, i.e., for a high percentage of overlapping areas. However, low values of the handover dwell time become very likely when the residual margin is quite low. Nonetheless, in most cases results obtained from the model have shown a good agreement with simulations.

The practical insights of the paper can be focused on an efficient design of handover procedures, which accounts for both the initiation and the execution phases. In particular, if the residual margin is high enough, queue-based prioritization schemes could benefit of quite long waiting times. To this respect, future work will concern the extension of the proposed approach to other initiation algorithms. Moreover, a further study should address the link between the overlapping area percentage in the cellular coverage and the protection degree of handover schemes.

APPENDIX A

Starting from the geometrical model depicted in Fig. 1 and denoting by (x, y) the coordinates of the generic crossing point Q between the outer circle and the direction of motion, the following two equations can be written:

$$x^2 + y^2 = R_2^2 \tag{A1}$$

$$y = P(x - R_1) \tag{A2}$$

where $P = \tan(\Theta)$. In particular, the last expression is the equation of the straight line through the points Q and H, the latter point having coordinates $(R_1, 0)$ and belonging to the handover threshold circumference.

By inserting (A2) in (A1), the following equation results:

$$(1 + P^2)x^2 - 2P^2R_1x + \left(P^2R_1^2 - R_2^2\right) = 0. \tag{A3}$$

By observing that values of Θ that actually lead to a MT leaving the cell are in the range $[-\frac{\pi}{2}, \frac{\pi}{2}]$, the following solution of (A3) is to be considered of interest:

$$x = \frac{P^2R_1 + \sqrt{R_2^2(1+P^2) - P^2R_1^2}}{1+P^2}. \tag{A4}$$

By inserting (A4) in (A2), y can be expressed as

$$y = P\left[\frac{P^2R_1 + \sqrt{R_2^2(1+P^2) - P^2R_1^2}}{1+P^2} - R_1\right] \tag{A5}$$

and substituting (A4) and (A5) into (4), it finally results

$$\Delta^2 = \frac{R_2^2(1+P^2) + R_1^2(1-P^2) - 2R_1\sqrt{R_2^2(1+P^2) - R_1^2P^2}}{1+P^2}. \tag{A6}$$

APPENDIX B

Moving from the described analysis of large excursions, the modeling of the handover dwell-time distribution presented in Section III-B can be completed as it follows:

$$f_{T_d}(t_d) = \begin{cases} \frac{f_{T_2}(t_d+\bar{t}_1)}{\int_{\bar{t}_1}^{\infty} f_{T_2}(\zeta)\,d\zeta}\left[1 - \int_0^{\bar{t}_1} f_{T_2}(\zeta)\,d\zeta\right] \\ \quad + f_{\bar{T}}(t_d)\int_0^{\bar{t}_1} f_{T_2}(\zeta)\,d\zeta, & \text{if } 0 \le t_d \le \bar{t}_{\max} \\ \frac{f_{T_2}(t_d+\bar{t}_1)}{\int_{\bar{t}_1}^{\infty} f_{T_2}(\zeta)\,d\zeta}\left[1 - \int_0^{\bar{t}_1} f_{T_2}(\zeta)\,d\zeta\right], & \text{if } t_d > \bar{t}_{\max} \end{cases} \tag{B1}$$

where $\int_0^{\bar{t}_1} f_{T_2}(\zeta)\,d\zeta$ is the probability of down crossing $Q_2(t)$ during the interval $[0, \bar{t}_1]$, i.e., the probability of observing a large excursion in that interval.

By inserting the expression of $f_{\bar{T}}(t_d)$, given in (27), the following expression results after some manipulations:

$$f_{T_d}(t_d) = \begin{cases} f_{T_2}(t_d+\bar{t}_1) \\ \quad + \int_0^{\bar{t}_1} f_{\bar{T}|T_2}(t_d \mid \zeta) f_{T_2}(\zeta)\,d\zeta, & \text{if } 0 \le t_d \le \bar{t}_{\max} \\ f_{T_2}(t_d+\bar{t}_1), & \text{if } t_d > \bar{t}_{\max}. \end{cases} \tag{B2}$$

From the approximation (B3), given at the bottom of the page, with $k_{\max} = \lfloor \bar{t}_{\max}/T \rfloor$ (where $\lfloor x \rfloor$ represents the lower integer part of x) and taking $p_{T_2}(iT) \cong T f_{T_2}(iT)$, (B4) follows, as given at the bottom of the page.

Moreover, from (18) it is obtained

$$p_{T_2}[(k_d + k_0)T] = P_{1,u}[(k_d + k_0 - 1)T] \prod_{j=0}^{k_d+k_0-2} \{1 - P_{1,u}(jT)\} \tag{B5}$$

where $P_{1,u}(kT)$ denotes, as (19), the probability of down crossing once the level $u = Q_{\text{th}}$ within the time interval $[kT, (k+1)T)$.

$$p_{T_d}(k_dT) \cong \begin{cases} T f_{T_2}[(k_d + k_0)T] \\ \quad + T\int_0^{\bar{t}_1} f_{\bar{T}|T_2}(k_dT \mid \zeta) f_{T_2}(\zeta)\,d\zeta, & \text{if } k_d = 1, \cdots, k_{\max} \\ T f_{T_2}[(k_d + k_0)T], & \text{if } k_d = k_{\max} + 1 \\ & \quad k_{\max} + 2, \cdots \end{cases} \tag{B3}$$

$$p_{T_d}(k_dT) \cong \begin{cases} p_{T_2}[(k_d + k_0)T] \\ \quad + T\int_0^{\bar{t}_1} f_{\bar{T}|T_2}(k_dT \mid \zeta) f_{T_2}(\zeta)\,d\zeta, & \text{if } k_d = 1, \cdots, k_{\max} \\ p_{T_2}[(k_d + k_0)T], & \text{if } k_d = k_{\max} + 1, \\ & \quad k_{\max} + 2, \cdots. \end{cases} \tag{B4}$$

Authorized licensed use limited to: Indraprastha Institute of Information Technology. Downloaded on December 09,2023 at 08:17:43 UTC from IEEE Xplore. Restrictions apply.

In order to provide an operative formula, the integral in (B4) is approximated by the area of a staircase function

$$\int_0^{\bar{t}_1} f_{\bar{T}|T_2}(k_dT \mid \zeta) f_{T_2}(\zeta)\, d\zeta \cong \sum_{j=0}^{k_0} f_{\bar{T}|T_2}(k_dT \mid jT) p_{T_2}(jT) \tag{B6}$$

so that (31) finally results.

ACKNOWLEDGMENT

The authors wish to thank the anonymous reviewers for their comments.

REFERENCES

[1] R. Vijayan and J. M. Holtzman, "A model for analyzing handoff algorithms," *IEEE Trans. Veh. Technol.*, vol. 42, no. 3, pp. 351–356, 1993.
[2] D. Hong and S. S. Rappaport, "Traffic model and performance analysis for cellular mobile radio telephone systems with prioritized and nonprioritized handoff procedures," *IEEE Trans. Veh. Technol.*, vol. 35, no. 3, pp. 77–92, 1986.
[3] S. Tekinay and B. Jabbari, "A measurement-based prioritization scheme for handovers in mobile cellular networks," *IEEE J. Select. Areas Commun.*, vol. 10, no. 8, pp. 1343–1350, 1992.
[4] R. Steele and M. Nofal, "Teletraffic performance of microcellular personal communications networks," *Proc. Inst. Elect. Eng.*, vol. 139, pt. I, no. 4, pp. 448–461, 1992.
[5] L. R. Hu and S. S. Rappaport, "Micro-cellular communications systems with hierarchical macrocell overlays: Traffic performance models and analysis," *Proc. IEEE*, vol. 82, no. 9, pp. 1383–1397, 1994.
[6] D. Giancristofaro, M. Ruggieri, and F. Santucci, "Analysis of queue-based handover procedures for mobile communications," in *Proc. IEEE ICUPC'93*, Ottawa, Canada, Oct. 1993, pp. 168–172.
[7] D. Giancristofaro, M. Ruggieri, and F. Santucci, "Queueing of handover requests in microcell network architectures," in *Proc. IEEE VTC'94*, Stockholm, Sweden, June 1994, pp. 1846–1849.
[8] M. Ruggieri, D. Giancristofaro, F. Graziosi, and F. Santucci, "An optimizable guard-channel based handover procedure for mobile microcellular systems," in *Proc. IEEE PIMRC'95*, Toronto, Canada, Sept. 1995, pp. 1357–1361.
[9] Y. B. Lin, S. Mohan, and A. Noerpel, "Queueing priority channel assignment strategies for PCS hand-off and initial access," *IEEE Trans. Veh. Technol.*, vol. 43, no. 3, pp. 704–712, 1994.
[10] S. S. Kuek, W. C. Wong, R. Vijayan, and D. J. Goodman, "A predictive load-sharing scheme in a microcellular radio environment," *IEEE Trans. Veh. Technol.*, vol. 42, no. 4, pp. 519–525, 1993.
[11] R. A. Guerin, "Channel occupancy time distribution in a cellular radio system," *IEEE Trans. Veh. Technol.*, vol. 35, no. 3, pp. 89–99, 1987.
[12] M. Ruggieri, F. Graziosi, and F. Santucci, "Characterization of the handover dwell time in mobile cellular networks," in *Proc. IEEE GLOBECOM'95*, Singapore, Nov. 1995, pp. 499–503.
[13] ——, "A model of the handover dwell time in mobile cellular systems," in *Proc. IEEE ICUPC'95*, Tokyo, Japan, Nov. 1995, pp. 364–368.
[14] M. Gudmundson, "Correlation model for shadow fading in mobile radio systems," *Electron. Lett.*, vol. 27, no. 23, pp. 2145–2146, 1991.
[15] A. Papoulis, *Probability, Random Variables, and Stochastic Processes*. New York: McGraw-Hill, 1965.
[16] N. Zhang and J. M. Holtzman, "Analysis of handoff algorithms using both absolute and relative measurements," in *Proc. IEEE VTC'94*, Stockholm, Sweden, June 1994, pp. 82–87.
[17] G. N. Senarath and D. Everitt, "Comparison of alternative handoff strategies for micro-cellular mobile communication systems," in *Proc. IEEE VTC'94*, June 1994, pp. 1465–1469.
[18] H. Cramér and M. R. Leadbetter, *Stationary and Related Stochastic Processes*. New York: Wiley, 1967.
[19] R. Vijayan and J. M. Holtzman, "Analysis of handoff algorithms using nonstationary signal strength measurements," in *Proc. IEEE GLOBECOM'92*, Orlando, FL, Dec. 1992, pp. 1405–1409.
[20] A. J. Rainal, "Bandwidth from a large excursion of Gaussian noise," *IEEE Trans. Instrum. Meas.*, vol. 40, no. 4, pp. 688–693, 1991.
[21] S. Nanda, "Teletraffic models for urban and suburban microcells: Cell sizes and handoff rates," *IEEE Trans. Veh. Technol.*, vol. 42, pp. 673–682, Nov. 1993.
[22] M. Gudmundson, "Analysis of handover algorithms," in *Proc. IEEE VTC'91*, St. Louis, MO, May 1991, pp. 537–542.
[23] W. H. Press, B. P. Flannery, S. A. Teukolsky, and W. T. Vetterling, *Numerical Recipes*. Cambridge, U.K.: Cambridge Univ. Press, 1986.

Marina Ruggieri (S'84–M'85–SM'94) was born in Naples, Italy, in 1961. She received the laurea degree in electronics engineering (*cum laude*) in 1984 at the University of Roma La Sapienza, Rome, Italy.

She was with FACE-ITT in the High Frequency Division from 1985 to 1986. She was trained on GaAs monolithic design and fabrication techniques at GTC-ITT, Roanoke, VA. She was a Research and Teaching Assistant at the Electronics Engineering Department, University of Roma Tor Vergata, from 1986 to 1991. She was an Associate Professor of Signal Theory at the Electrical Engineering Department, University of L'Aquila, L'Aquila, Italy, from 1991 to 1994. Since 1994, she has been Associate Professor of Digital Signal Processing at the University of Roma Tor Vergata. Her research activities mainly concern terrestrial and satellite systems for mobile communications. She has participated in feasibility studies committed by the European Space Agency. She is presently working on handover procedures for mobile microcellular networks, wideband wireless local-area networks, satellite system requirements, and reliability issues.

Mrs. Ruggieri was awarded the 1990 Piero Frati International Prize for *A New Millimeter Wave Satellite System for Land Mobile Communications*, which was also coauthored by Prof. F. Valdoni, A. Paraboni, and F. Vatalaro.

Fabio Graziosi (S'96–M'97) was born in L'Aquila, Italy, in 1968. He received the laurea and doctoral degrees in electronic engineering from the University of L'Aquila, L'Aquila, in 1993 and 1997, respectively.

Since February 1997, he has been an Assistant Professor in Telecommunications at the Department of Electrical Engineering, University of L'Aquila. His present research interests involve mobility management and multiple-access techniques for personal communication systems.

Dr. Graziosi received one of the prizes for the 40th Fondazione Ugo Bordoni for his thesis work in 1994.

Fortunato Santucci (S'93–M'95) was born in L'Aquila, Italy, in 1964. He received the laurea and Ph.D. degrees in electronic engineering from the University of L'Aquila, L'Aquila, in 1989 and 1994, respectively.

In 1989, he was with Selenia Spazio S.p.a., Rome, Italy, working on VSAT networks design. From 1991 to 1992, he was at the Solid State Electronics Institute (I.E.S.S.) of the National Research Council (C.N.R.), Rome, doing research on superconductor receivers for millimeter-wave satellite systems. Since 1994, he has been an Assistant Professor in Telecommunications at the Department of Electrical Engineering, University of L'Aquila. In 1996, he was a Visiting Researcher at the Department of Electrical and Computer Engineering, University of Victoria, B.C., Canada, where he did research on CDMA networks. His current research activity is focused on mobility management, traffic modeling, and multiple-access techniques for mobile radio communications networks.

Authorized licensed use limited to: Indraprastha Institute of Information Technology. Downloaded on December 09,2023 at 08:17:43 UTC from IEEE Xplore. Restrictions apply.